Gene Expression Changes in Residual Advanced Cervical Cancer after Radiotherapy: Indicators of Poor Prognosis and Radioresistance?

Authors' Contribution:
Study Design **A**
Data Collection **B**
Statistical Analysis **C**
Data Interpretation **D**
Manuscript Preparation **E**
Literature Search **F**
Funds Collection **G**

BC 1   **Zhi-chao Fu***
A 2   **Feng-mei Wang***
AG 3   **Jian-ming Cai**

1 Department of Radiotherapy, Fu Zhou General Hospital, Fuzhou, Fujian, P.R. China
2 Department of Obstetrics and Gynecology, Fu Zhou General Hospital, Fuzhou, Fujian, P.R. China
3 Department of Radiation Medicine, Faculty of Naval Medicine, Second Military Medical University, Shanghai, P.R. China

Corresponding Author:
Source of support:

* Zhi-chao Fu and Feng-mei Wang contributed to this article equally
Jian-ming Cai, e-mail: carnation1112@163.com
Departmental sources

Background: Different sensitivity of advanced cervical cancer to irradiation can decrease effectiveness of radiotherapy in some cases. We attempted to identify the differentially expressed genes in residual cervical cancer after radiotherapy that might be associated with poor prognosis and radioresistance.

Material/Methods: Differential genes expression was identified by an oligonucleotide microarray in cervical cancer tissues before radiation and after a 50-Gy dose of radiation. The microarray results were validated by quantitative real-time PCR. CXCL12 was validated by immunohistochemistry in paraffin-embedded cervical cancer tissues before radiotherapy. The relationship between the differentiated gene and prognosis was validated by survival analysis.

Results: Hierarchic cluster analysis identified 238 differentiated genes that exhibited ≥3.0-fold change and p<0.05. We found 111 genes that were in persistent up-regulation and 127 in persistent down-regulation after a 50-Gy dose of radiation when compared with the control group. These genes were involved in processes such as cell growth and death, cell-apoptosis, cell cycle regulation, cell signaling, DNA synthesis and repair, and cell adhesion. High differential expression of CXCL12, CD74, FGF7, COL14A1, PRC1, and RAD54L genes was validated by quantitative PCR before and after radiotherapy. Survival analysis results showed that the high expression of CXCL12 was closely related to poor prognosis.

Conclusions: The higher expression of CXCL12 might be informative regarding poor prognosis in patients undergoing radical radiotherapy. The differentially expressed genes identified in our study might provide a new method for diagnosis and treatment of radioresistance in cervical cancer.

MeSH Keywords: **Chemokine CXCL12 • Prognosis • Radioligand Assay • Transcriptome**

Full-text PDF: http://www.medscimonit.com/abstract/index/idArt/893689

📄 2698   ⊞ 7   📊 5   📚 22

Background

Cervical cancer, the second most common cancer in women, occurs around the world. It has a high incidence and mortality, especially in middle- and low-income countries. The number of cervical cancer cases is estimated to have increased by 14% from 2000 to 2005 in China [1]. Although the 5-year overall survival rate of advanced cervical cancer patients has increased with the development of radiotherapy and chemotherapy, radioresistance and metastasis are still the difficulties for radiation oncologists because tumors, even with similar pathological pattern and stage, are not equally sensitive to radiation. Some studies had shown that radiation therapy is closely related to gene susceptibility [2,3]. Several radioresistance-associated genes such as HIF-1 and p53 had been investigated, but the exact mechanism of radioresistance is not known. Thus, identifying the molecular basis of cervical cancer radioresistance is of vital importance and may lead to novel radiosensitive strategies.

In this study, we investigate the differential expression genes in the tumor tissues before and after radiotherapy by the whole human genome oligo microarray. The expression level of the differential expression genes was performed by hierarchical clustering. We also analyzed the potential functions of the interested genes. We screened-out a list of genes that might be closely related to radioresistance and the related pathways by above methods. Our results may provide targets for the development of radiosensitive drugs and set individualized treatment for advanced cervical cancer.

Material and Methods

Patients and treatment

From January 2005 to October 2007, 135 women with cervical squamous cell carcinoma were treated with radiotherapy at the Department of Radiotherapy, Fuzhou General Hospital. Patients without integrated follow-up were excluded. A total of 130 patients had undergone whole-course radiotherapy were included in this study. Approval by the Institutional Review Board of Fu Zhou General Hospital was obtained in advance, and the informed consent requirement was waived because the current study was performed by retrospective review, but the informed consent of the other 3 patients with staged IIIB in 2012 was obtained because the data of these patients were analyzed prospectively. None of the enrolled patients had underlying disease that would influence survival.

Patients with advanced cervical cancer (stage IIB-IVA) underwent radiotherapy. The radiotherapy protocols included a 30Gy whole pelvic irradiation and a subsequent 20 Gy central shield irradiation. The total dose of intracavity irradiation to Point A was 36-48 Gy. Concurrent chemoradiation was conducted by 2 cycles of platinum-based chemotherapy in all patients. The radiotherapy protocols were performed according to the NCCN guideline (2004). The machines were Varian600C/D medical linear accelerators.

We obtained the tumor samples prior to radiotherapy by punch biopsy. The samples were fixed in 10% formalin and embedded in paraffin. The paraffin-embedded sections were cut into 5-mm sections and processed for H+E staining, as well as histochemical and immunohistochemical studies. Residual tumor tissues of 3 patients undergoing a total 50 Gy dose of radiotherapy were also obtained by punch biopsy. One part of these tumor tissues was used for RNA detection and the other part was processed the same as in pre-radiotherapy.

The patients were followed up every 3 months in the first 2 years, every 6 months in the third year, and every year afterwards. Imageological, ultrasonic, and blood examinations were performed to observe local recurrence at every follow-up. International Federation of Gynecology and Obstetrics (FIGO) staging system were used to evaluate the clinical staging. The retrospective research data were obtained from hospital records.

Total RNA extraction and oligonucleotide array sequence analysis

Total RNA was extracted from tumor tissues of 3 patients before radiotherapy and residual tumor tissues after a total radiotherapy dose of 50 Gy obtained by punch biopsy using TRIZOL Reagent (Cat#15596-018, Life Technologies, Carlsbad, CA, US) following the manufacturer's instructions and checked for an RIN number to inspect RNA integrity by an Agilent Bioanalyzer 2100. The integrity of all RNA samples was verified with 2100 RIN $\geq$7.0 and 28S/18S $\geq$0.7. Qualified total RNA was further purified by use of the RNeasy micro kit (Cat#74004, QIAGEN, GmBH, Germany) and RNase-Free DNase Set (Cat#79254, QIAGEN, GmBH, Germany).

The samples were amplified, labeled, and purified by using GeneChip 3'IVT Express Kit (Cat#901229, Affymetrix, Santa Clara, CA, USA) followed the manufacturer's instructions to obtain biotin-labeled cDNA. Array hybridization and washing was performed using GeneChip® Hybridization, Wash and Stain Kit (Cat#900720, Affymetrix, Santa Clara, CA, USA) in a Hybridization Oven 645 (Cat#00-0331-220V, Affymetrix, Santa Clara, CA, USA) and Fluidics Station 450 (Cat#00-0079, Affymetrix, Santa Clara, CA, USA) following the manufacturer's instructions. Slides were scanned by a GeneChip® Scanner 3000 (Cat#00-00212, Affymetrix, Santa Clara, CA, US) and Command Console Software 3.1 (Affymetrix, Santa Clara, CA,

Table 1. Primer pairs for qRT-PCR.

Gene name	Gene bank ID	Primer sequence from 5' to 3'	Product length (bp)
CXCL12	NM_199168	F-gattcttcgaaagccatgttg R-cactttagcttcgggtcaatg	136
CD74	NM_004355	F-gaatgctgaccccctgaaggtgta R-gggggctgaagggagcaagaaagc	396
FGF7	NM_002009	F-ggatccatgcaatgacatgactccaga R-aagcttaagttattgccataggaagaaagtggg	507
COL14A1	NM_021110	F-gcgaattccagcagcagggccggct R-ggctcgagtcacatggggactggg	480
PRC1	NM_003981	F-gccaacaaggagaacctgga R-tctcgctgaagcccaacag	167
RAD54L	NM_001142548	F- gacctttggctcatgggtact R- caggacctgccttcaggttt	106

US) with default settings. Raw data were normalized by RMA algorithm, Gene Spring Software 11.0 (Agilent Technologies, Santa Clara, CA, US).

Quantitative real-time PCR

To validate the results of microarray data, real-time PCR was performed. Six genes were used as an internal control: CXCL12, CD74, FGF7, COL14A1, PRC1, and RAD54L. Primer sequences used for real-time PCR are shown in Table 1.

PCR was performed as follows: 95°C for 5 min; 40 cycles of 95°C for 30 s, annealing temperature 56–58°C for 90 s, and 72°C for 60 s. The PCR products were separated on a 2% agarose gel, visualized with ethidium bromide staining, and photographed with FAS-III Series (NIPPON Genetics Co., Ltd., Tokyo, Japan). We used the MiniOpticon Real-Time PCR Detection System (Bio-Rad, Hercules, CA) for real-time PCR. Relative quantification of PCR products was calculated after normalization to β-actin.

Histochemical and immunohistochemical analyses

Xylene was used to deparaffinize the tissue blocks sections. The sections were then rehydrated in a descending ethanol series. Finally, they were rinsed with water and incubated for 30 min in 0.3% hydrogen peroxide in methanol. The serial sections were incubated with primary anti-CXCL12 in a humid chamber at 4°C overnight. They were then rinsed in PBS, and incubated for 1 h with a horseradish peroxidase-conjugated secondary antibody.

Immunohistologic expression was assessed by 2 expert pathologists independently without knowledge of clinical outcome. The positive cell degree was expressed using a scale from 0 to 4: (–) represents 0%; (+) represents 1–25%; (++) represents 26–50%; (+++) represents 51–75%, and (++++) represents 76–100%.

Table 2. Patients' characteristics.

Characteristics	N (%)	
Age (year)		
<50	53	(40.8)
>50	77	(59.2)
Stage (FIGO)		
IIb	33	(25.4)
III	58	(44.6)
Iva	39	(30.0)
Tumor size		
<4 cm	53	(40.8)
>4 cm	77	(59.2)
Tumor classification		
Exogenous	35	(26.9)
Endogenous	30	(23.1)
Cervical canal	30	(23.1)
Ulcerative	35	(26.9)
Adjuvant therapy		
None	59	(45.4)
Concurrent chemoradiation	71	(54.6)

We conducted survival analysis on 130 patients. The length of time from the date of radiotherapy ending to the date of death or the last follow-up was defined as the overall survival (OS) time.

Statistical analyses

SPSS 18.0 for windows were performed. Survival was estimated using the Kaplan-Meier method. We used the log-rank

This work is licensed under a Creative Commons
Attribution-NonCommercial-NoDerivs 3.0 Unported License

1278

Indexed in: [Current Contents/Clinical Medicine] [SCI Expanded] [ISI Alerting System]
[ISI Journals Master List] [Index Medicus/MEDLINE] [EMBASE/Excerpta Medica]
[Chemical Abstracts/CAS] [Index Copernicus]

Table 3. Sample qualification.

Sample ID	A260/ A280	RIN	28S/18S	Result
1	1.93	6.0	0.8	Part degradation
1*	1.89	7.7	1.4	Qualified
2	1.86	7.7	1.3	Qualified
2*	1.97	7.2	1.4	Qualified
3	1.87	7.3	1.0	Qualified
3*	1.97	7.1	1.0	Qualified

1*,2*,3* means tumor tissues before radiotherapy; 1, 2, 3 means tumor tissues after 50 Gy dose of radiation of the corresponding patient.
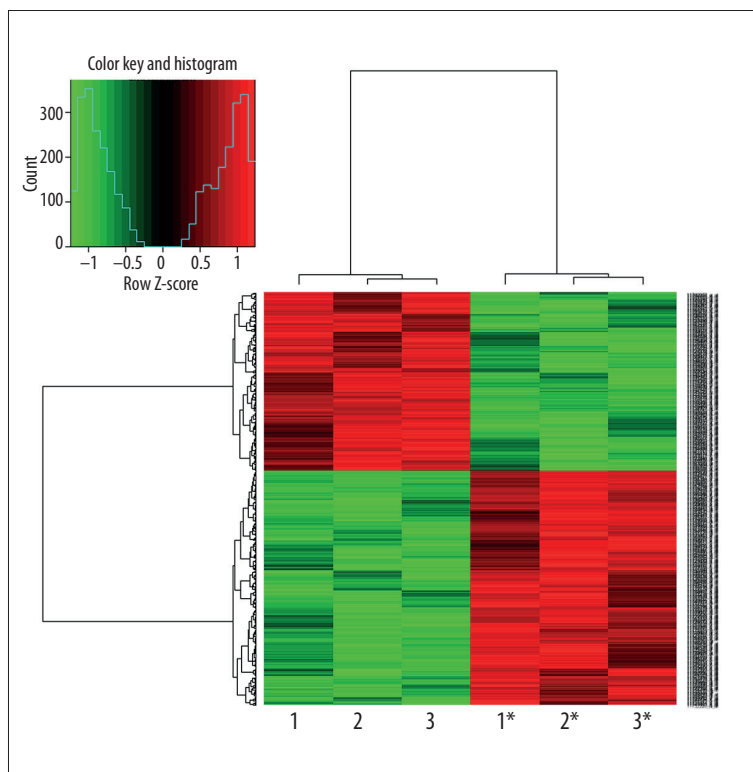

Figure 1. Hierarchical clustering map of differential gene expression. The result of hierarchical clustering on conditions shows a distinguishable gene expression profiling among samples. 1*, 2*, 3* means tumor tissues before radiotherapy; 1, 2, 3 means tumor tissues after a 50-Gy dose of radiation of the corresponding patient.

test to analyze the factors of survival time for any significant differences. Predictors of clinical radioresistance were identified by logistic regression analysis. Cox's regression analysis was used to calculate the prognostic significance of individual parameters. The χ^2 test and Fisher's exact test were used to evaluate differences in proportions. When the P value was below 0.05, the difference was considered to be significant.

Results

Patients' characteristics

The characteristics of 130 patients are listed in Table 2. The mean patient age was 53.7, ranging from 35 to 78. The median follow-up time in surviving patients was 68 months.

Table 4. Up-regulated genes in the residual cervical cancer after 50 Gy dose of radiation at least fivefold higher.

Gene_symbol	GenBank accession	Description	Foldchange	P values
CXCL12	NM_199168	Chemokine (C-X-C motif) ligand 12	34.37257	0.0051
FYB	NM_199335	FYN binding protein	21.33432	0.0065
LOC100506582	XR_109454	Uncharacterized LOC100506582	19.26455	0.0038
PTGDS	NM_000954	Prostaglandin D2 synthase 21kDa (brain)	18.24440	0.0049
CHI3L2	NM_004000	Chitinase 3-like 2	17.63723	0.0090
COL14A1	NM_021110	Collagen, type XIV, alpha 1	15.4829	0.0001
SNED1	NM_001080437	Sushi, nidogen and EGF-like domains 1	11.93017	0.0094
PTPRC	NM_002838	Protein tyrosine phosphatase, receptor type, C	11.76348	0.0080
BHLHE22	NM_152414	Basic helix-loop-helix family, member e22	11.05505	0.0072
HLA-DQA1	NM_002122	Major histocompatibility complex, class II, DQ alpha 1	10.89394	0.0039
MGST1	NM_001260511	Microsomal glutathione S-transferase 1	10.68159	0.0056
IQGAP2	NM_006633	IQ motif containing GTPase activating protein 2	10.67557	0.0052
FGF7	NM_002009	Fibroblast growth factor 7	10.11275	0.0047
MRC1	NM_001009567	Mannose receptor, C type 1	9.53875	0.0042
CASP1	NM_001223	Caspase 1, apoptosis-related cysteine peptidase	8.89591	0.0086
TRIM22	NM_006074	Tripartite motif containing 22	8.77551	0.0094
CD74	NM_004355	CD74 molecule, major histocompatibility complex, class II invariant chain	8.52676	0.0062
SELE	NM_000450	Selectin E	8.26213	0.0015
HLA-DPB1	NM_002121	Major histocompatibility complex, class II, DP beta 1	7.91193	0.0040
IRAK3	NM_007199	Interleukin-1 receptor-associated kinase 3	7.88364	0.0098
IGDCC4	NM_020962	Immunoglobulin superfamily, DCC subclass, member 4	7.52929	0.0005
KCTD12	NM_138444	Potassium channel tetramerisation domain containing 12	7.47977	0.0099
HLA-DMB	NM_002118	Major histocompatibility complex, class II, DM beta	6.91416	0.0076
PTGFR	NM_001039585	Prostaglandin F receptor (FP)	6.90784	0.0063
SAMD4A	NM_015589	Sterile alpha motif domain containing 4A	6.86448	0.0048
VWCE	NM_152718	von Willebrand factor C and EGF domains	6.77407	0.0003
MMP2	NM_004530	Matrix metallopeptidase 2 (gelatinase A, 72kDa gelatinase, 72kDa type IV collagenase)	6.69944	0.0042
CAPN3	NM_173088	Calpain 3, (p94)	6.54548	0.0086
RASA4	NM_001079877	RAS p21 protein activator 4	6.49581	0.0020
CELF2	NM_001025076	CUGBP, Elav-like family member 2	6.44033	0.0062
FNBP1	NM_015033	Formin binding protein 1	5.88967	0.0067

Table 4 continued. Up-regulated genes in the residual cervical cancer after 50 Gy dose of radiation at least fivefold higher.

Gene_symbol	GenBank accession	Description	Foldchange	P values
FLI1	NM_002017	Friend leukemia virus integration 1	5.78461	0.0038
ZMAT1	NM_001011657	Zinc finger, matrin-type 1	5.73992	0.0009
MICAL1	NM_022765	Microtubule associated monoxygenase, calponin and LIM domain containing 1	5.67725	0.0059
C1orf38	NM_004848	Chromosome 1 open reading frame 38	5.55259	0.0097
ARPC4-TTLL3	NM_015644	Tubulin tyrosine ligase-like family, member 3	5.52604	0.0016
IFFO1	NM_001193457	Intermediate filament family orphan 1	5.44289	0.0062
EPB41L3	NM_012307	Erythrocyte membrane protein band 4.1-like 3	5.38832	0.0049
PPM1K	NM_152542	Protein phosphatase, Mg2+/Mn2+ dependent, 1K	5.30152	0.0069
BIRC3	NM_182962	Baculoviral IAP repeat containing 3	5.26144	0.0018
PRKCB	NM_212535	Protein kinase C, beta	5.22640	0.0065
CREBRF	NM_153607	CREB3 regulatory factor	5.21976	0.0033
CLIC2	NM_001289	Chloride intracellular channel 2	5.16835	0.0052
AMICA1	NM_153206	Adhesion molecule, interacts with CXADR antigen 1	5.14923	0.0099
GAS6	NM_000820	Growth arrest-specific 6	5.12683	0.0048

Gene expression analysis and clustering

Microarray quality control verified the expression of all the samples to be qualified (Table 3). The differential expression genes were identified by hierarchical clustering map analysis (Figure 1). There were 111 up-regulated and 127 down-regulated genes among a total of 238 differentiated genes that exhibited ≥3.0-fold change and p<0.05 were identified with 111 up-regulated and 127 down-regulated (Tables 4, 5).

Quantitative RT-PCR validate the gene expression results

As shown in Figure 2, Tables 1 and 6 highly differentially expressed genes – CXCL12, CD74, FGF7, COL14A1, PRC1, and RAD54L – were selected to verify the microarray results. These results were highly correlated with the microarray data. The above data strongly supported the reliability of the microarray results.

Validation of protein expression and analysis of the relationship between CXCL12 expression and survival rate

We detected the expression of CXCL12 protein with immunohistochemistry on 130 paraffin-embedded samples. The gene expression results were confirmed at the protein level. Immunolocalization with anti-CXCL12 antibody largely showed positive staining in the cell membrane and cytoplasm of cancer cells (Figure 3). The CXCL12 positive cell ratio was 61.5%. No correlation was found between the expression of CXCL12 and several clinicopathological factors, including age, sex, FIGO stage, tumor size, and treatment program (Table 6). We found that CXCL12 was an independent risk factor by Kaplan-Meier survival analysis. CXCL12 was strongly correlated with a poor prognosis. The death risk ratio of patients with positive CXCL12 expression to negative expression is 3.07. There was a significant difference between the groups (p=0.035) (Figure 4, Table 7).

Expression of CXCL12 in tumor tissues before radiotherapy and residual tumor tissues after a radiotherapy dose of 50 Gy

RNA was extracted from tumor tissues of 5 patients with stage IIIB cervical cancer before radiotherapy and after a radiotherapy dose of 50 Gy. The expression of CXCL12 was detected. As shown in Figure 5, the increasing mRNA expression of CXCL12 occurred in residual tissues with the ratio of 35.3.

Discussion

Radiation therapy is an effective radical approach for advanced cervical cancer; however, not every patient has good response to irradiation, which might be an important cause

Table 5. Down-regulated genes in the residual cervical cancer after 50 Gy dose of radiation at least fourfold higher.

Gene_symbol	GenBank accession	Description	Foldchange	*P* values
MEST	NM_177525	Mesoderm specific transcript homolog (mouse)	19.03931	0.0008
CDKN3	NM_001130851	Cyclin-dependent kinase inhibitor 3	15.72590	0.0079
HES6	NM_001142853	Hairy and enhancer of split 6 (Drosophila)	13.30584	0.0035
CENPN	NM_001100624	Centromere protein N	13.19284	0.0010
CDC6	NM_001254	Cell division cycle 6 homolog (*S. cerevisiae*)	12.67188	0.0002
MCM10	NM_018518	Minichromosome maintenance complex component 10	12.42256	0.0043
MND1	NM_001253861	Meiotic nuclear divisions 1 homolog (*S. cerevisiae*)	12.38095	0.0067
ZNF367	NM_153695	Zinc finger protein 367	12.13090	0.0004
GINS1	NM_021067	GINS complex subunit 1 (Psf1 homolog)	11.95449	0.0011
PRC1	NM_003981	Protein regulator of cytokinesis 1	11.78833	0.0099
KIAA0101	NM_014736	KIAA0101	11.48251	0.0079
ESCO2	NM_001017420	Establishment of cohesion 1 homolog 2 (*S. cerevisiae*)	11.18837	0.0085
FAM64A	NM_019013	Family with sequence similarity 64, member A	10.46812	0.0044
TMEM97	NM_014573	Transmembrane protein 97	10.36410	0.0046
STMN1	NM_203401	Stathmin 1	9.814851	0.0012
MLF1IP	NM_024629	MLF1 interacting protein	9.786415	0.0005
TK1	NM_003258	Thymidine kinase 1, soluble	9.528579	0.0014
E2F7	NM_203394	E2F transcription factor 7	9.295376	0.0050
BIRC5	NM_001012270	Baculoviral IAP repeat containing 5	9.246912	0.0082
GINS2	NM_016095	GINS complex subunit 2 (Psf2 homolog)	9.024759	0.0030
FAM111B	NM_001142703	Family with sequence similarity 111, member B	8.962451	0.0034
ORC6	NM_014321	Origin recognition complex, subunit 6	8.926719	0.0050
GGH	NM_003878	Gamma-glutamyl hydrolase (conjugase, folylpolygammaglutamyl hydrolase)	8.558582	0.0071
CDC45	NM_001178010	Cell division cycle 45 homolog (*S. cerevisiae*)	8.505507	0.0098
PXMP2	NM_018663	Peroxisomal membrane protein 2, 22kDa	8.168918	0.0096
CDT1	NM_030928	Chromatin licensing and DNA replication factor 1	7.987140	0.0047
RNASEH2A	NM_006397	Ribonuclease H2, subunit A	7.735180	0.0001
CHML	NM_001821	Choroideremia-like (Rab escort protein 2)	7.648427	0.0001
FANCI	NM_001113378	Fanconi anemia, complementation group I	7.272155	0.0044
EXO1	NM_003686	Exonuclease 1	6.787611	0.0037
RFC4	NM_002916	Replication factor C (activator 1) 4	6.678417	0.0062
C1orf112	NM_018186	Chromosome 1 open reading frame 112	6.629925	0.0022
KLHL23	NM_001199290	Kelch-like 23 (Drosophila)	6.565550	0.0088

Table 5 continued. Down-regulated genes in the residual cervical cancer after 50 Gy dose of radiation at least fourfold higher.

| Gene_symbol	GenBank accession	Description	Foldchange	P values
ATAD2	NM_014109	ATPase family, AAA domain containing 2	6.412012	0.0074
CCNE1	NM_001238	Cyclin E1	6.285823	0.0003
KIF15	NM_020242	Kinesin family member 15	6.28417	0.0096
MCM4	NM_005914	Minichromosome maintenance complex component 4	6.21293	0.0065
DSCC1	NM_024094	Defective in sister chromatid cohesion 1 homolog (*S. cerevisiae*)	6.19047	0.0099
TMEM106C	NM_001143841	Transmembrane protein 106C	6.01842	0.0073
HOMER1	NM_004272	Homer homolog 1 (Drosophila)	5.89936	0.0095
CHEK1	NM_001114121	Checkpoint kinase 1	5.67529	0.0003
RAD51C	NM_002876	RAD51 homolog C (*S. cerevisiae*)	5.62493	0.0020
MIS18A	NM_018944	MIS18 kinetochore protein homolog A (*S. pombe*)	5.61498	0.0074
BRCA1	NM_007294	Breast cancer 1, early onset	5.51289	0.0061
MSH2	NM_000251	MutS homolog 2, colon cancer, nonpolyposis type 1 (E. coli)	5.40957	0.0082
RFC5	NM_001130112	Replication factor C (activator 1) 5, 36.5kDa	5.40903	0.0081
VRK1	NM_003384	Vaccinia related kinase 1	5.38942	0.0011
CCDC58	NM_001017928	Coiled-coil domain containing 58	5.38923	0.0072
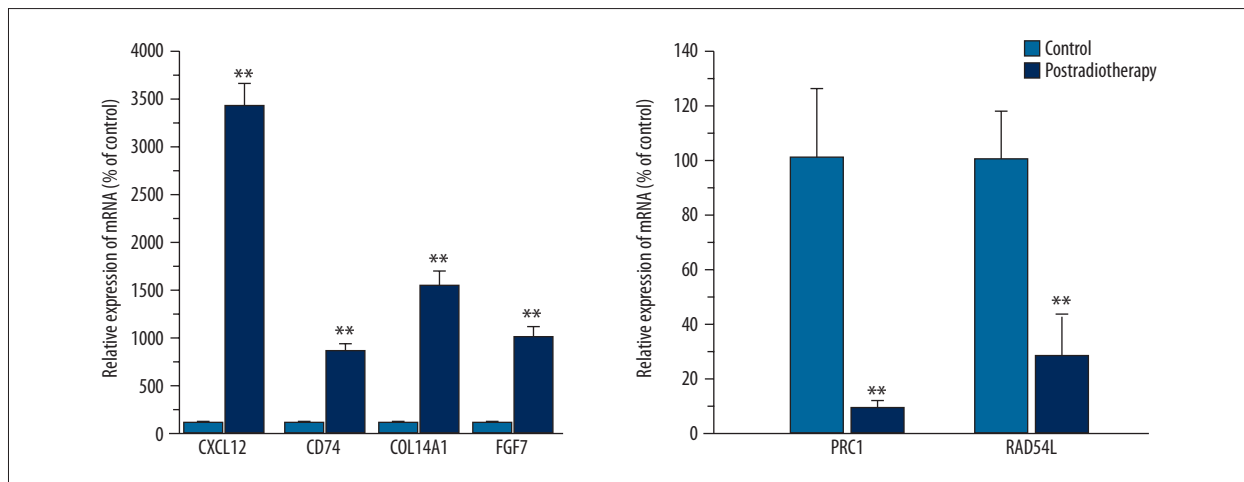
Figure 2. Quantitative real-time PCR validation of the microarray data. All qRT-PCR data were generally consistent with cDNA microarray data. The relative expression of CXCL12, CD74, COL14A1, and FGF was significantly higher in residual cervical cancer after a 50-Gy dose of irradiation. The relative expression of PRC1 and RAD54L was significantly lower in tumor tissues after radiotherapy. QRTPCR was done in triplicate and the ratio was calculated relative to the reference genes b-action.** $P<0.05$ versus control.

of local recurrence or metastasis. Thus identifying the radioresistance-associated genes and making individual radiotherapy schedules could enhance the clinical outcomes. High-density oligonucleotide and cDNA microarrays, which are the high-throughput technologies for assaying gene expression, may identify the differential expression of genes in tumor tissues
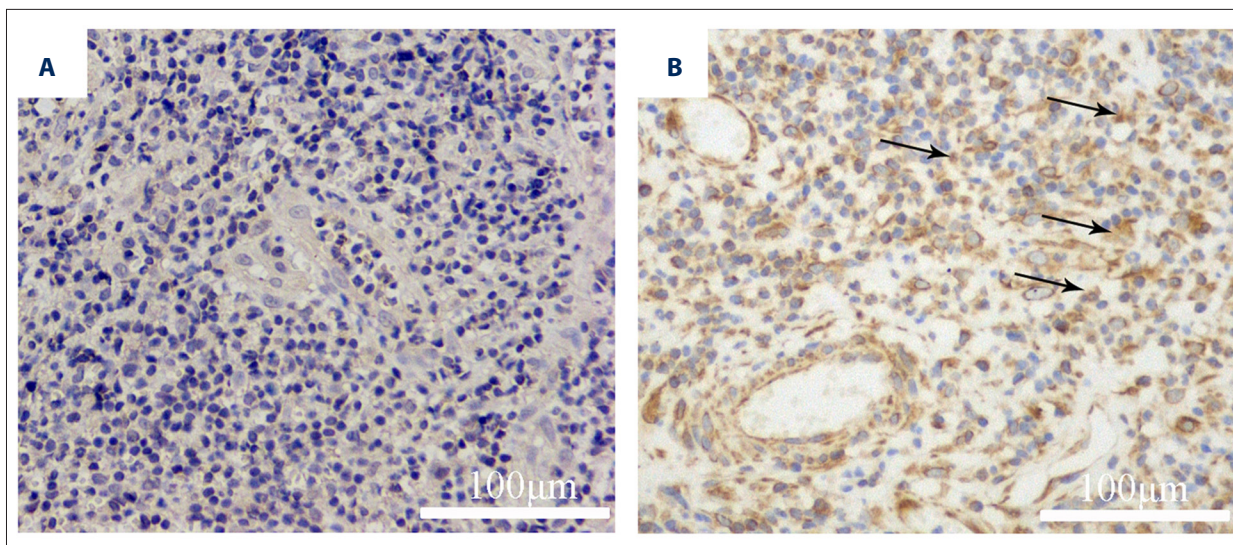
Figure 3. Immunohistochemical staining of CXCL12. A. CXCL12 (brown) expression (++++) in the cell membrane and cytoplasm of cancer cells (×200). B. CXCL12 (brown) expression (+) in the cell membrane and cytoplasm of cancer cells (×200).

Table 6. Correlation between CXCL12 expression and clinicopathological factors in cervical cancer of 130 patients.

| | CXCL12 | | P |
	Positive	Negative	
Age (years)			0.343
<50	27	21	
>50	53	29	
FIGO stage			0.449
II	22	14	
III	31	24	
IV	27	12	
Tumor size			0.512
<4 cm	34	19	
>4 cm	45	32	
Treatment			0.504
Radiotherapy	34	25	
CCRT	45	26	

before and after radiotherapy. In this study, we revealed 127 highly differentially expressed genes involved in processes such as cell cycling, cell apoptosis, cell signaling, and cell adhesion. The changed expression genes of residual tumor tissues-derived may mean high metastasis and radioresistance in cervical cancer.

The chemokine family is among the significantly differentially expressed genes that participate in tumor growth and metastasis [4]. CXCL12, a member of a superfamily of small pro-inflammatory chemoattractant cytokines, was first cloned from

a bone marrow-derived stromal cell line. Several studies have shown that CXCL12 expression was correlated with poor prognosis in various cancers such as breast cancer, lung cancer, colorectal cancer, and endometrial cancer [5–7]. DNA-damaging agents such as irradiation or chemotherapeutics could increase CXCL12 expression. Wolff et al. found that the CXCL12 expression had significant alternations in head and neck squamous cell carcinoma cell lines after X-ray irradiation [8]. Shu-Chi Wang et al. [9] found that a significant increase in CXCL12 expression occurred at 24 h after irradiation in murine astrocytoma tumor cell lines and also found that radiotherapy could
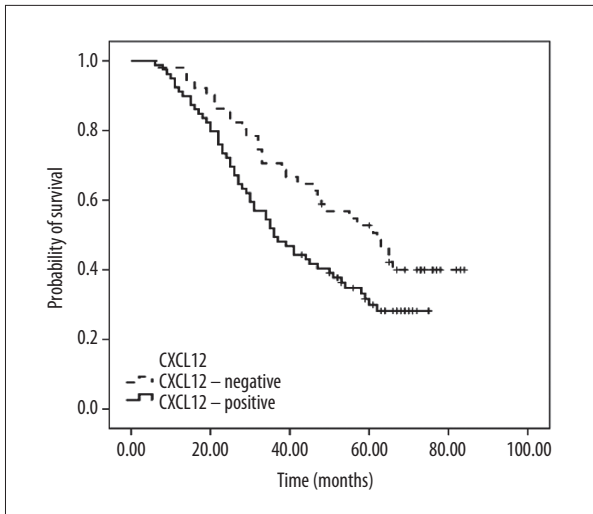
Figure 4. Kaplan-Meier survival analysis of patients with advanced cervical cancer. Kaplan-Meier survival analysis shows that the positive expression of CXCL12 is an independent risk factor in patients with advanced cervical cancer and strongly correlates with poor prognosis.
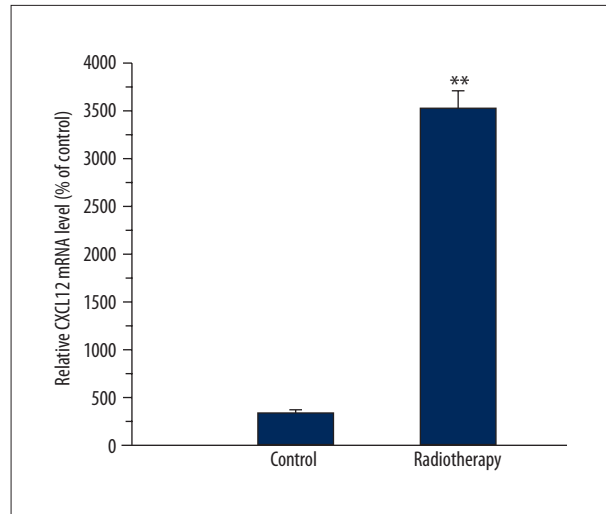

Figure 5. Real-time RT-PCR analysis of the expression of CXCL12 in advanced cervical cancer before and after a dose of radiotherapy. Expression of CXCL12 mRNA was measured with quantitative real-time PCR and normalized to b-actin mRNA expression. A significant increasing expression of CXCL12 mRNA was observed in residual cervical cancer. ** $p<0.01$ compared to tumor tissues before radiation therapy.

Table 7. Univariate and multivariate Cox regression analysis of prognostic factors.

Clinicopathological characteristics	n (n=130)	5-year survival rate	Kaplan-Meier analysis		Cox regression model analysis	
			χ^2	P-value	χ^2	P-value
Age (years)						
<40	48	31.6				
≥40	82	44.0	2.284	0.131	0.147	0.702
FIGO stage						
II b	36	53.5				
III	55	40.6				
IV a	39	25.2	8.108	0.017	6.272	0.012
Tumor size						
<4 cm	53	41.2				
≥4 cm	77	39.3	0.432	0.511	0.228	0.633
Treatment						
Radiotherapy	59	28.4				
CCRT	71	48.1	5.983	0.014	5.423	0.020
CXCL12 expression						
Positive	79	30.0				
Negative	51	52.7	4.305	0.038	4.451	0.035

CCRT – concurrent chemoradiation.

increase the microvascular density (MVD) and the CXCL12 expression of shrunken brain tumor tissues after a dose of 8 Gy or 15 Gy. They thought these results indicated that local brain irradiation effectively reduced the growth rate of the primary tumor, but promoted tumor invasiveness. These factors might increase the complexity of gliomas following radiation therapy.

Similar to their results, we also found that the expression of CXCL12 increased significantly in residual tumor tissues after an irradiation dose of 50 Gy. We found that CXCL12 was an independent risk factor by a Kaplan-Meier survival analysis. CXCL12 was strongly correlated with a poor prognosis. In our opinion, the mechanism of CXCL12 in radioresistance might be as follows: CXCL12 might be a bidirectional cue that attracted T cells at low concentrations and repelled them at high concentrations [10]. When a dose of irradiation increased the expression of CXCL12, this chemotactic factor might repel the T cells, inducing the tumor invasion; at the same time, the increased expression of CXCL12 induced the tumor angiogenesis. Alternatively, irradiation could increase the expression of HIF-1α, which is highly expressed in hypoxia. The CXCL12 promoter contains 2 HIF-1α binding sites, thus increasing the expression of HIF-1α results in the elevation of CXCL12 levels. Hypoxia can induce the dedifferentiation and stemness of cancer cells [11]. CXCL12 has the ability to mediate the survival and proliferation of human progenitor cells. Thus, we though that CXCL12 might mediate the homing of cancer stem cells with the characteristics of radioresistance.

CXCR4, expressed by several cells, is believed as the specific chemokine receptor of CXCL12. The CXCL12/CXCR4 axis plays an important role in tumor growth, metastasis, and angiogenesis. Recently, CXCR7 had also been demonstrated to be another receptor for CXCL12 and to predict poor disease-free and disease-specific survival in cervical cancer patients [12]. Thus, there were questions about whether CXCL12 played roles in radioresistance by binding CXCR4 or CXCR7 or both. Another question concerns the signal pathway. In future research we expect to address these questions. Interestingly, we did not find differential expression of CXCR4 or CXCR7 between the tumor tissues before and after radiotherapy, perhaps because irradiation could increase the expression of CXCL12 rather than the expression of its receptors, CXCR4 or CXCR7. Another possibility might be that there was no significant statistical difference between the expression of CXCR4 or CXCR7 before and after radiotherapy.

ATM, firstly described in 1995, was defective in patients with ataxia-telangiectasia. This disease is characterized by cancer susceptibility and profound sensitivity to ionizing radiation [13]. ATM, a central kinase involved in the cellular response to DNA double-strand breaks that can lead to the cancer development, could arise when the cells are exposed to ionizing radiation. ATM could regulate DNA damage-induced G2/M cell cycle arrest, which is necessary for DNA repair after irradiation. As this hypersensitivity of ATM-defective cells to ionizing radiation, ATM has drawn research attention as a therapeutic factor for cancer therapy. Several inhibitors of ATM with different limitations have been reported. KU-60019, an ATP-competitive ATM inhibitor reported by Golding et al. [14]

in 2009, possessed greater potency as a radiosensitizer. They also reported that this ATM inhibitor alone was not toxic for normal brain tissues outside the radiation field. KU-59403, another ATM inhibitor reported by Batey et al. in 2013, also possessed potency as a radiosensitizer and exhibited greater solubility and bio-availability than KU-60019 [15]. Although they have significant potency as radiosensitizers, none of these ATM inhibitors are in clinical development at present. In this study, an up-regulated ATM was observed in the residual tumor tissues after radiotherapy. We thought that the increased expression of the ATM gene might play a radioresistant role in advanced cervical cancer.

Proteinases, which are secreted molecules, could degrade various components of the extracellular matrix. Matrix metalloproteinases (MMPs), a kind of proteinase, play an important role in tumor invasion and metastasis via their proteolytic activity. Several studies have shown that irradiation could alter the proteinase activity in tumor cells and tissues [16,17]. MMP-2 belongs to MMPs, which takes part in extracellular matrix degradation. Up-regulations of MMP-2 in different irradiation conditions have been found in glioblastoma, as well as in colorectal and lung cancer, which leads to enhanced cell invasion [18–20]. Park et al. [21] found that MMP-2, enhanced by irradiation, was involved in irradiation-induced invasion of glioma cells. Chetty et al. [22] also showed that irradiation could increase MMP-2 protein expression and activity in lung cancer cells and that inhibition of MMP-2 could enhance the radiosensitivity. In their study, down-regulation of MMP-2 in the irradiated cells prevented the induction of the FOXM1-mediated DNA repair gene. An up-regulation of MMP-2 was also found in residual cervical cancer tissues after a dose of irradiation in this study. Thus, our results suggested that combined-therapy of MMP-2 inhibitors and irradiation might provide a more effective treatment for advanced cervical cancer.

Path analysis identified some signal pathways in response to irradiation, including cell growth and death, differentiation, cells adhesion and extracellular matrix, Wnt-signaling pathway, TGF-beta signaling pathway, and other signaling pathways that play important roles in tumorigenesis, progression, and invasion. However, the mechanisms of these genes in radiotherapy of advanced cervical cancer still need much clarification.

Conclusions

In this study, we identified dozens of genetic changes in advanced cervical cancer tissues after a dose of irradiation; some of them might be responsible for enhanced metastasis and radioresistance. We found 111 up-regulated genes and 127 down-regulated genes. In future research we plan to validate the functionality of these identified genes. Further research

might provide a theoretical basis to develop more effective approaches to improve the radiosensitivity of advanced cervical cancer.

References:

1. Yang L, Parkin DM, Ferlay J et al: Estimates of cancer incidence in China for 2000 and projections for 2005. Cancer Epidemiol Biomarkers Prev, 2005; 14: 243–50

2. Peltenburg LT: Radiosensitivity of tumor cells. Oncogenes and apoptosis. Q J Nucl Med, 2000; 44: 355–64

3. Awasthi S, Singhal SS, Yadav S et al: RLIP76 is a major determinant of radiation sensitivity. Cancer Res, 2005; 65: 6022–28

4. Muralidhar GG, Barbolina MV: Chemokine receptors in epithelial ovarian cancer. Int J Mol Sci, 2013; 15: 361–76

5. Dehghani M, Kianpour S, Zangeneh A et al: CXCL12 Modulates prostate cancer cell adhesion by altering the levels or activities of β1-containing integrins. Int J Cell Biol, 2014; 2014: 981750

6. Bajetto A, Barbieri F, Pattarozzi A et al: CXCR4 and SDF1expression in human meningiomas: a proliferative role in tumoral meningothelial cells *in vitro*. Neuro Oncol, 2007; 9: 3–11

7. Fridrichova I, Smolkova B, Kajabova V et al: CXCL12 and ADAM23 hypermethylation are associated with advanced breast cancers. Transl Res, 2015; pii: S1931-5244(14)00470-8

8. Wolff HA, Rolke D, Rave-Fränk M et al: Analysis of chemokine and chemokine receptor expression in squamous cell carcinoma of the head and neck (SCCHN) cell lines. Radiat Environ Biophys, 2011; 50: 145–54

9. Wang SC, Yu CF, Hong JH, Tsai CS, Chiang CS: Radiation therapy-induced tumor invasiveness is associated with SDF-1-regulated macrophage mobilization and vasculogenesis. PLoS One, 2013; 8(8): e69182

10. Jaafar F, Righi E, Lindstrom V et al: Correlation of CXCL12 expression and FoxP3+ cell infiltration with human papillomavirus infection and clinicopathological progression of cervical cancer. Am J Pathol, 2009; 175(4): 1525–35

11. Li P, Zhou C, Xu L, Xiao H: Hypoxia enhances stemness of cancer stem cells in glioblastoma: an *in vitro* study. Int J Med Sci, 2013; 10(4): 399–407

12. Schrevel M, Karim R, ter Haar NT et al: CXCR7 expression is associated with disease-free and disease-specific survival in cervical cancer patients. Br J Cancer, 2012; 106(9): 1520–25

13. Savitsky K, Bar-Shira A, Gilad S et al: A single ataxia telangiectasia gene with a product similar to PI-3 kinase. Science, 1995; 268(5218): 1749–53

14. Golding SE, Rosenberg E, Valerie N et al: Improved ATM kinase inhibitor KU-60019 radiosensitizes glioma cells, compromises insulin, AKT and ERK prosurvival signaling, and inhibits migration and invasion. Mol Cancer Ther, 2009; 8: 2894–902

15. Batey MA, Zhao Y, Kyle S et al: Preclinical evaluation of a novel ATM inhibitor, KU59403, *in vitro* and *in vivo* in p53 functional and dysfunctional models of human cancer. Mol Cancer Ther, 2013; 12: 959–67

16. Asuthkar S, Velpula KK, Nalla AK et al: Irradiation-induced angiogenesis is associated with an MMP-9-miR-494-syndecan-1 regulatory loop in medulloblastoma cells. Oncogene, 2014; 33(15): 1922–33

17. Maddirela DR, Kesanakurti D, Gujrati M et al: MMP-2 suppression abrogates irradiation-induced microtubule formation in endothelial cells by inhibiting αvβ3-mediated SDF-1/CXCR4 signaling. Int J Oncol, 2013; 42(4): 1279–88

18. Qian LW, Mizumoto K, Urashima T et al: Radiationinduced increase in invasive potential of human pancreatic cancer cells and its blockade by a matrix metalloproteinase inhibitor, CGS27023. Clin Cancer Res, 2002; 8(4): 1223–27

19. Lee WH, Warrington JP, Sonntag WE et al: Irradiation alters MMP-2/TIMP-2 system and collagen type IV degradation in brain. Int J Radiat Oncol Biol Phys, 2012; 82(5): 1559–66

20. Speake WJ, Dean RA, Kumar A et al: Radiation induced MMP expression from rectal cancer is short lived but contributes to *in vitro* invasion. Eur J Surg Oncol, 2005; 3(8): 869–74

21. Park MH, Ahn BH, Hong YK et al: Overexpression of phospholipase D enhances matrix metalloproteinase-2 expression and glioma cell invasion via protein kinase C and protein kinase A/NF-kappaB/Sp1-mediated signaling pathways. Carcinogenesis, 2009; 30(2): 356–65

22. Chetty C, Bhoopathi P, Rao JS et al: Inhibition of matrix metalloproteinase-2 enhances radiosensitivity by abrogating radiation-induced FoxM1-mediated G2/M arrest in A549 lung cancer cells. Int J Cancer, 2009; 124(10): 2468–77

Conflict of interest

We declare that we have no conflicts of interest.